Atmos. Chem. Phys. Discuss., 7, 12035–12066, 2007
www.atmos-chem-phys-discuss.net/7/12035/2007/

Atmospheric Chemistry and Physics Discussions

Comparison between the first Odin-SMR, Aura MLS and CloudSat retrievals of cloud ice mass in the upper tropical troposphere

P. Eriksson[1], M. Ekström[1], B. Rydberg[1], D. L. Wu[2], R. T. Austin[3], and D. P. Murtagh[1]

[1]Department of Radio and Space Science, Chalmers University of Technology, Gothenburg, Sweden
[2]Jet Propulsion Laboratory, California Institute of Technology, Pasadena, California, USA
[3]Department of Atmospheric Science, Colorado State University, Fort Collins, Colorado, USA

Received: 17 July 2007 – Accepted: 10 August 2007 – Published: 14 August 2007

Correspondence to: P. Eriksson (patrick.eriksson@chalmers.se)

Abstract

Emerging microwave satellite techniques are expected to provide improved global measurements of cloud ice mass. CloudSat, Aura MLS and Odin-SMR fall into this category and first cloud ice retrievals from these instruments are compared. The comparison is made for partial ice water columns above 12 km, following the SMR retrieval product. None of the instruments shows significant false cloud detections and a consistent view of the geographical distribution of cloud ice is obtained, but differences on the absolute levels exist. CloudSat gives the lowest values, with an overall mean of 2.12 g/m^2. A comparable mean for MLS is 4.30 g/m^2. This relatively high mean can be an indication of overestimation of the vertical altitude of cloud ice by the MLS retrievals. The vertical response of SMR has also some uncertainty, but this does not affect the comparison between MLS and CloudSat. SMR observations are sensitive to cloud inhomogeneities inside the footprint and some compensation is required. Results in good agreement with CloudSat, both in regard of the mean and probability density functions, are obtained for a weak compensation, while a simple characterisation of the effect indicates the need for stronger compensation. The SMR mean was found to be 1.89/2.62/4.10 g/m^2 for no/selected/strongest compensation, respectively. Assumptions about the particle size distribution are a consideration for all three instruments, and constitute the dominating retrieval uncertainty for CloudSat. The comparison indicates a retrieval accuracy of about 40% (3.1±1.2 g/m^2). This number is already very small compared to uncertainties of cloud ice parametrisation in atmospheric models, but can be decreased further through a better understanding of main retrieval error sources.

1 Introduction

The circulation of water through the atmosphere is key to the Earth's climate system, but this branch of the hydrological cycle is still not fully understood due to its complex-

ity and measurement system limitations. Traditional satellite observation techniques largely fail at providing information on the internal structure of ice clouds and knowledge around the tropospheric cloud ice component is particularly poor. There is not even a consistent view upon such a basic variable as the vertically integrated cloud ice mass, often denoted as the ice water path (IWP). For example, the zonal mean IWP in climate models used in the 4th assessment of the Intergovernmental Panel on Climate Change differs with up to one order of magnitude, and the IWP response to increasing levels of CO_2 deviates in sign (John and Soden, 2006).

Satellite techniques are needed to obtain the geographical and temporal coverage required for running and validating global atmospheric models. The climate is driven by fluxes of optical and IR radiation and satellite observations in these wavelengths regions are important for understanding cloud radiative forcing. Morphological data, such as occurrence frequency and cloud top altitude are also obtained, but information on micro-physical properties is restricted to thinner clouds or the cloud top layer (e.g. Dessler and Yang, 2003). This as the scattering of optical and IR radiation by cloud particles is strong.

Further considerations regarding the cloud penetration capability, the strength of atmospheric gaseous absorption and that the measured signal should be generated by interaction with particles carrying a dominating fraction of the cloud ice mass, indicate that mm and sub-mm technologies are the most suitable for characterising the bulk properties of thicker clouds (Evans and Stephens, 1995; Evans et al., 1998). The relative importance of observations at different wavelengths depends on the atmospheric conditions, the technology selected (active or passive) and the observation geometry (down-looking or limb sounding). Cloud ice absorption is relatively low at mm and sub-mm wavelengths, and clouds affect the measured radiation mainly through scattering.

Meteorological microwave satellite sensors, such as AMSU-B, are so far restricted to frequencies below 190 GHz and down-looking geometry. Only the largest cloud ice particles cause significant scattering for these observation conditions, and data of AMSU-B type have primarily been used to identify deep convection at tropical latitudes

(Hong et al., 2005). Limb sounding offers longer propagation paths through the atmosphere and this results in detectable cloud ice radiance signatures already at lower frequencies. Ice water content (IWC) retrievals based on 203 GHz radiances were presented for UARS MLS (Wu et al., 2005), the first satellite microwave limb sounder launched in 1991.

Remaining microwave limb sounders, Odin-SMR (launched 2001) and Aura MLS (launched 2004), are both in operation, and are also the only other examples of satellite observations in the frequency range above 200 GHz. Based on the good experience from UARS MLS, IWC retrievals were a design target of Aura MLS, and promising initial results involving validation of atmospheric models have already been presented (Li et al., 2005, 2007; Su et al., 2006a,b). These results are based on observations at 240 GHz, but unofficial results from 115, 190 and 640 GHz also exist (Wu et al., 2006). The operational Odin-SMR processing covers strato- and mesospheric altitudes, but an off-line dual frequency (501/544 GHz) retrieval approach for deriving humidity and a partial IWP product for the tropical upper troposphere has been presented recently (Ekström et al., 2007; Eriksson et al., 2007a). Similar comparisons with ECMWF and climate models in Li et al. (2005) and Eriksson et al. (2007a) indicate on overall agreement between Odin-SMR and Aura MLS cloud mass retrievals, while a first direct comparison of the datasets is presented here.

Active techniques provide cloud observations with much higher spatial resolution than the passive methods discussed above. Lidars, being a optical/IR method, perform best for thinner clouds. Radars do not have this limitation, but require high frequency pulses or large antennas to obtain sensitivity to cloud ice particles. Two ground-based networks of such radars exist: ARM (www.arm.gov) and CloudNet (www.cloud-net.org). CloudSat, launched 2006 and operating at 94 GHz, is the first space-borne radar of this type, and signifies a very important step forward in global remote sensing of clouds (Stephens et al., 2002). The first CloudSat ice mass retrievals have just been made released as a provisional product (R03).

It can then be expected that global measurements of cloud ice masses are now

performed with improved accuracy, and by three different sensors. However, important retrieval uncertainties still exist and different validation efforts are needed. This paper contributes to these efforts by investigating the consistency between first official version of Odin-SMR, Aura MLS and CloudSat IWC/IWP retrievals. Special attention is put on Odin-SMR as this is the first comparison study of this dataset. Aura MLS and CloudSat are also compared in Wu et al. (2007)[1], but then in a broader context and using an Aura MLS data version in production. Some aspects of main retrieval uncertainties are also emphasised here.

A main consideration for all present satellite techniques is that assumptions about the particle size distribution must be made in order to retrieve cloud ice masses. This introduces a substantial retrieval uncertainty as the particle distribution changes with local atmospheric conditions (Heymsfield and McFarquhar, 2002) and no parametrisation of general validity exists. A second main retrieval error source for instruments with poorer spatial resolution, such as Odin-SMR and Aura MLS, is that the cloud ice is not homogeneously distributed over the antenna footprint. This problem increases with the degree of non-linearity between cloud ice mass and observed signal. Different cloud ice masses, averaged over the footprint, can then cause the same signal, depending on the spatial distribution. This is known as the beam filling effect, and has been studied for Aura MLS by Davis et al. (2006).

2 Data

This section describes datasets involved. The aim is to compare first official cloud ice mass retrievals from three satellite microwave sensor presently in operation: Odin-SMR, Aura MLS and CloudSat. Ground-based radar observations from the Atmospheric Radiation Measurement program are used for further reference. The comparison follows the characteristics of the Odin-SMR retrieval approach and all data are analysed as the partial ice water path defined by Fig. 1. That is, only ice above about 11 kmis considered and a natural limitation to tropical latitudes is imposed.

[1] Wu, D. L., Jiang, J. H., Read, W. G., Austin, R. T., Davis, C. P., Lambert, A., Kahn, B. H., Nankervis, C. J., Sneep, M., Veefkind, J. P., Pumphrey, H. C., Stephens, G. L., Tanelli, S., Vane, D. G., and Waters, J. W.: Validation of Aura MLS cloud ice water content (IWC) measurements, J. Geophys. Res., submitted, 2007.

2.1 Odin-SMR

2.1.1 Observations

The Odin satellite was launched in February 2001 into a ∼600 km quasi-polar sun-synchronous orbit, with ascending node around 18:00 h. The payload includes the first space-borne sensor for atmospheric sub-mm observations, Odin-SMR. This limb sounding instrument measures thermal emission at frequencies around 500 GHz. The atmospheric signal is recorded through a 1.1 m telescope, single-sideband heterodyne receivers and two auto-correlation spectrometers with 800 MHz bandwidth. Further information is found in, for example, Murtagh et al. (2002) and Ekström et al. (2007).

The observation time of Odin is timeshared, both between astronomy and atmospheric science objectives, and between different atmospheric observation modes. Cloud ice retrievals are based on radiances from the stratospheric mode, measurements made approximately every third day. The data set includes 2.0×10^5 retrievals, covering the period 24 July 2001–20 April 2007, and can be obtained through www.rss.chalmers.se/~patrick/OdinUT.

2.1.2 Retrieval approach

Operational Odin-SMR processing does not account for cloud scattering and data are here taken from the separate retrieval algorithm presented by Eriksson et al. (2007a). These retrievals consider only spectra from tangent altitudes below 9 km, where the atmosphere around the tangent point acts as blackbody background to cloud scattering at higher altitudes. Clouds are then detected by a depression of recorded brightness

temperatures, ΔT_b. The measurement strategy is accordingly more of down-looking character and the footprint size is relatively small, compared to pure limb sounding geometry. The sampled volume is a tilted cylinder, where the horizontal cross-section has an area of about $2 \times 45\,km^2$.

The observation geometry selected provides no inherent altitude information, but this problem is partly overcome by combining data from 501 and 544 GHz. This procedure results in the retrieval of a partial IWP, with an estimated response to cloud ice at different altitudes shown in Fig. 1. This retrieval product is below denoted as pIWP.

The mapping from derived ΔT_b values to pIWP relies on the particle size distribution of McFarquhar and Heymsfield (1997) and radiative transfer calculations made for completely homogeneous cloud layers (1-D). The simple correction for cloud inhomogeneity (beam filling) suggested in Eriksson et al. (2007a) is applied, but with new parameter values derived below in Sect. 3.2.

2.2 Aura MLS

2.2.1 Observations

Aura MLS is a passive instrument consisting of seven radiometers at frequencies near 118, 190, 240, 640 GHz, and 2.5 THz (Waters et al., 2006). The 118 GHz and 2.5 THz radiometers have two receivers at orthogonal polarisations. The 118 GHz receivers are single-sideband, while at other frequencies double-sideband systems are employed. The Aura satellite has a 13:40 ascending node sun-synchronous orbit at 705 km altitude with 98° inclination. The MLS on Aura views forwards in the satellite flying direction with daily latitude coverage from 82° S to 82° N. The field of view at 240 GHz has a vertical size of ≈3.2 km, and is ≈7 km in the cross-track dimension. MLS scans are synchronised to the orbital period such that nominal operation will have 240 limb scans per orbit. The data integration time for each measurement is 1/6 s. For GHz measurements, each scan includes 40–50 spectra dedicated to tropospheric measurements with a 300 m sampling resolution in tangent height (Jarnot et al., 2006).

The first official Aura MLS data product is denoted as version 1.5 and is used here. The newer V2.2 was avoided as this data set is not yet complete. Most importantly, the time period for which CloudSat data are at hand has not yet been processed. This study is based on 1.0×10^6 IWC profiles, spanning the period 8 August 2004–14 February 2007 in a continuous manner.

2.2.2 Retrieval approach

The V1.5 IWC data product is based on measurements around 240 GHz and covers altitudes above the 261 hPa level. Only usage of data above 215 hPa is recommended, but as the conversion to Odin-SMR pIWP (Fig. 1) puts little weight below 215 hPa possible retrieval problems at 261 hPa should be of relatively small importance. The officially suggested screening and bias correction of data (Wu et al., 2006) has been performed.

The fundamental quantity for Aura MLS cloud ice retrievals is the difference between measured and expected clear-sky radiance, named as the cloud-induced radiance T_{cir}. This is basically the same quantity as the Odin-SMR ΔT_b, but there are some important practical differences. First of all, T_{cir} is determined as part of the operational processing, where the estimation of clear-sky radiance incorporates retrieval information from other bands and T_{cir} should be more accurately determined than ΔT_b. Further, the Aura MLS retrievals are made at higher tangent altitudes, and at a frequency with comparably low optical thicknesses. This causes relevant T_{cir} values to be strictly positive.

Derived V1.5 T_{cir} values are mapped to IWC in a linear manner, as described in Wu et al. (2006). This approach causes a systematic underestimation of IWC at large values, where the relationship between T_{cir} and IWC is non-linear. The effect of this non-linearity has been addressed in the V2.2 data version that replaced V1.5 in March 2007. An initial study has found that V2.2 yields better IWC results, particularly at pressures ≤ 261 hPa (Wu et al., 2007[1]). Both V1.5 and V2.2 IWC retrievals assume the PSD of McFarquhar and Heymsfield (1997), as for Odin-SMR.

2.3 CloudSat

2.3.1 Observations

CloudSat is a satellite mission designed to measure the vertical structure of clouds from space (Stephens et al., 2002). The satellite flies in tandem with Aura, and has accordingly the same orbit properties. CloudSat carries a 94 GHz 0.16° off-nadir looking radar which measures the power backscattered by clouds as a function of distance from the radar. The standard data product consists of 125 vertical bins that are 240 m thick, while the vertical resolution of the radar is approximately 500 m. Each profile is generated over a 160 ms integration, with a footprint resolution of approximately 1.4 km across-track and 2.5 km along track. The minimum detectable equivalent radar reflectivity is approximately –30 dBZ and the dynamic range is 70 dBZ. IWC profiles from the 2B-CWC-RO release 3 (R03) product for the period of 15 October 2006–15 November 2006 are considered. These are the only official CloudSat ice mass retrievals offered at this moment, providing 5.4×10^6 data points. The provisional R03 product should be replaced by an operational R04 product covering the full extent of the mission later during 2007.

2.3.2 Retrieval approach

The CloudSat 2B-CWC-RO R03 IWC product is retrieved from radar reflectivity measurements only. In this retrieval algorithm a gamma particle size distribution is assumed. Such a function can be completely characterised by three parameters: the width and slope of the distribution and the total number concentration of particles. The distribution width, number concentration, and profile of slope values are retrieved in an optimal estimation framework that uses a priori values based on a generic ice cloud case and the reflectivity level. The IWC can then be estimated based on the retrieved particle size distribution parameters. The retrieval approximates ice particles as spheres and applies a correction for Mie scattering.

2.4 Tropical ARM radars

The Atmospheric Radiation Measurement (ARM) program involves a number of highly instrumented ground stations for measuring parameters that determine the radiative properties of the atmosphere. Data from the Millimetre Wavelength Cloud Radars (MMCR) located at the tropical western Pacific sites Manus (2.006° S, 147.425° E) and Nauru (0.521° S, 166.916° E) are considered. The MMCR is a zenith-pointing radar that operates at a frequency of 35 GHz, and reports radar reflectivity of the atmosphere up to 20 km, with a vertical resolution of 90 m. From the Manus site data from 28 February 2003–14 December 2003, and from the Nauru site data from 8 January 2002– 2 February 2002 and 11 September 2003–14 December 2003 were obtained.

The scheme of Liu and Illingworth (2000) was applied for the mapping from dBZ to IWC. Reflectivity profiles are reported as 30 s mean values. A further averaging over 100 sequential corresponding IWC profiles was applied to create a dataset better matching the satellite measurements in respect of horizontal resolution.

3 Results and discussion

3.1 Particle size sampling

The interaction between radiation at a given wavelength and a cloud ice particle depends on the particle's size, shape and complex refractive index. The overall radiative impact of cloud ice inside a given volume depends further on the particle size distribution (PSD). These facts cause a remote sensing system to have a maximum sensitivity to a specific particle size range. If the purpose of the measurement is to estimate IWC or IWP, it is of course beneficial if the range of maximum sensitivity corresponds to ice particles carrying a large fraction of the ice mass.

This aspect is investigated by Fig. 2, for considered satellite observations and a characteristic infrared wavelength. The two cases selected roughly match the thinnest and

thickest clouds of relevance for considered data. Different cross-section components are considered, to best represent the properties of each measurement technique. The secondary maximum in MLS sensitivity functions around 50 µm corresponds to particle absorption, as shown by Fig. A1 in Wu et al. (2005). Absorption is neglected for Odin-SMR due to the different observation geometry applied. In short, absorption gives here a low radiative effect as absorbed energy is replaced with emission of similar strength, as described in Eriksson et al. (2007a).

Figure 2 confirms that IR radiation interacts primarily with smaller particles, while the microwave techniques are more sensitive to larger particles. The division line is found at a particle diameter of around 100 µm. For the "thin cloud" case, the area of highest response for the IR wavelength corresponds roughly to the lower half of the mass, while the microwave responses (MLS is discussed separately below) match approximately the upper third. The situation is reversed for the "thick cloud": 30/50% coverage but with a higher value for microwaves.

An interesting exception is MLS and the "thin cloud" case, where the response function shows a clear sensitivity to both small and large particles, caused by a combined effect of absorption and scattering. A more detailed sensitivity study would show an even higher relative response to small particles, as extinction due to absorption here influences measured spectra more strongly (with about a factor of 2). This indicates that MLS, in this aspect, is the most suitable choice here for measuring the ice mass in thinner clouds, again on the condition that a detectable signal is obtained.

The scattering for MLS and CloudSat is predominately of Rayleigh character. That is, the scattering strength is proportional to D^6, where D is the particle diameter. The relatively shorter wavelength of SMR results in a transition to Mie conditions at a smaller particle size, and this gives a lower relative response for particles above ~300 µm. This has the consequence that MLS and CloudSat retrievals are more easily affected by large particles above the PSD range important for the total mass, than for SMR. A combination of mm and sub-mm measurements has accordingly some potential for discriminating between medium sized and large particles. This particularly for higher

IWC and temperatures than considered here, but lower incidence angles than used for SMR are needed to maintain sensitivity at sub-mm wavelengths down to altitudes where such conditions are encountered.

Despite the features noted above, the overall responses of the microwave techniques are quite similar. The MH97 PSD (McFarquhar and Heymsfield, 1997) is assumed for both MLS and SMR retrievals. This has the consequence that no larger deviations will be caused between SMR and MLS retrievals even if MH97 would be a poor representation of mean state of true PSDs. CloudSat is independent on this point from SMR and MLS. It is impossible to judge, without detailed simulations, if the assumptions made for CloudSat lead to higher or lower retrieved ice masses.

However, on the assumptions that all involved instruments make a perfect retrieval and that the true PSD equals MH97, it can be determined that CloudSat (assuming a gamma pSD) would give a lower ice mass than MLS and SMR. MH97 divides the total PSD into two modes, one each for small and large particles. CloudSat has limited sensitivity to particles of the small mode, and the retrieval will, for the assumed conditions yield the mass held by the large mode. MLS and SMR retrievals will include the mass of the low mode, due to the a priori assumption of MH97, even if the measurement itself has no sensitivity to small mode particles.

3.2 Impact of cloud inhomogeneity

Cloud ice fields normally show horizontal inhomogeneities on scales matching the footprints of Aura MLS and Odin-SMR. This causes a beam filling effect (see introduction) as the relationship between cloud ice amount and measured signal is non-linear (see Fig. 6 in Wu et al. (2006) for MLS and Fig. 6 in Eriksson et al. (2007a) for SMR). A simple correction scheme for this cloud inhomogeneity effect was suggested for SMR in Eriksson et al. (2007a), based solely on simple arguments around the pIWP – ΔT_b relationship and data from a case study made by Davis et al. (2006).

The access to CloudSat data gives the possibility to quantify the beam filling effect, and the result of a simple analysis is given in Fig. 3. Synthetic Odin-SMR data were

generated by mapping time series of CloudSat pIWP to ΔT_b, and approximating the antenna response as a rectangular function spanning 30 sequential CloudSat data points. The mapping from pIWP to ΔT_b, denoted as f in figure axes labels, was taken from the retrieval lookup tables. The antenna response is denoted as r. Simulated SMR measurements are obtained as $r(f(\text{pIWP}))$. The retrieval assumes that pIWP averaged over the antenna footprint gives same ΔT_b. The later quantity is $f(r(\text{pIWP}))$.

Completely homogeneous ice fields are found at the diagonal of Fig. 3, while non-linear effects place inhomogeneous cases off the diagonal. Data points above the diagonal, only found for low ΔT_b, are caused by a non-linearity originating in the PSD. This effect was not foreseen by Eriksson et al. (2007a). The pIWP to ΔT_b mapping is further non-linear due to radiative transfer effects, and this feature is the origin to data points below the diagonal and would, if neglected, cause a systematic underestimation of pIWP. These effects can not be compensated on a single measurement basis, and the only option is to apply a general correction with the aim to obtain correct mean values.

The correction suggested in Eriksson et al. (2007a, Eq. 1) is included in Fig. 3 and it catches the properties of simulated results for higher pIWP. Considering the reversed effect discovered for low IWP, it was decided to not apply any correction for ΔT_b below 10 K. The breakpoint, between a linear increase of correction factor and a constant value, was then also moved up to 40 K (from 20 K) to avoid a too narrow transition region. Numerical tests showed that changes of the breakpoints inside realistic ranges have low influence, but the choice of maximum correction is critical. For example, the overall mean of the Odin-SMR data is 1.95, 2.69 and 4.19 g/m^2 for a maximum correction of 0, 10 and 20%, respectively. The choice of 20% was based on an expectation of throughout inhomogeneous conditions for high pIWP, but Fig. 3 contradicts this assumption (high number of points close to the diagonal). The maximum correction was decreased to 10% based on this observation. The updated correction function is displayed in Fig. 3.

Beam filling is also a relevant phenomenon for MLS, but probably with a smaller

impact. The relationship between ice mass and influence on measured spectra is approximately linear up to 30 g/m^2 for SMR, while the same applies for MLS up to ≈50 mg/m^3 (Wu et al., 2007[1]). Assuming an effective cloud thickness of 2 km for higher pIWP, this indicates a larger linear regime of MLS with a factor of around 3, which is advantageous with respect to beam filling.

3.3 Geographical distributions

CloudSat data are only available for a single month, and a comparison to seasonally matched Odin-SMR and Aura MLS data is found in Fig. 4. The Odin-SMR data set is comparably sparse, particularly for the part of the year of interest here. A broader seasonal window was then applied, but the statistical basis is still poorer for Odin-SMR than for the other instruments. SMR also provides the least smooth field of pIWP.

The geographical distribution is very similar between the instruments. Higher mean values are primarily found around the intertropical convergence zone (ITCZ), north-east parts of the Indian, western Pacific Ocean, central equatorial areas of Africa and South America. The south pacific convergence zone (SPCZ) can further be distinguished, but its southern end is not present for CloudSat. The presence of large areas, common for the instruments, with mean pIWP below 1 g/m^2 show that none of the instruments have a notable percentage of false cloud detections.

The match between local mean pIWP values is analysed further in Fig. 5. The spread of the data points is significant for all three instrument pairs, but smallest for the MLS – CloudSat due to the higher statistical noise in the SMR data. The data are best centred around the 1 – 1 line for SMR – CloudSat, while MLS gives higher pIWP, especially in comparison with CloudSat. The mean values are also 4.30, 3.08 and 2.12 g/m^2 for MLS, SMR and CloudSat, respectively. A difference between mean value of SMR and the other instruments can be caused by incorrect estimation of SMR's vertical response (Fig. 1). MLS and CloudSat IWC profiles are weighted with same vertical response and the only complication is that data are given as a function of pressure and altitude, respectively. Conversion between pressure and altitude should only cause

marginal uncertainty. However, the vertical resolution of MLS is relatively poor and there are indications on that cloud top altitudes are overestimated by about 1 km (Wu et al., 2007[1]). A test where MLS IWC profiles were shifted 1 km downwards gave a mean of 2.29 g/m^2, a value in good agreement to CloudSat. This would then leave SMR with a higher mean value, pointing towards an overcompensation for beam filling or that the sensitivity of the SMR measurements has been underestimated for lower altitudes.

The complete Odin-SMR and Aura MLS data sets are summarised in Figs. 6 and 7. The overall mean is 3.16 g/m^2 for SMR and 4.40 g/m^2 for MLS. The SMR fields appear also here as less smooth. This is mainly caused by a smaller volume of data for SMR, but differences in footprint size could further be of importance. Clear seasonal variations are seen. The variations are not discussed in detail here, but it is noted that the instruments show the same patterns. For example, the strongest SPCZ and the least pronounced ITCZ for the eastern Pacific Ocean appear during the DJF season in both cases. This shows again that the cloud identification is robust for both MLS and SMR, and cloud ice mass differences originate in the mapping from cloud induced radiances.

Further, the data sets give a consistent view of comparably high ice masses above areas of Africa and South America (Fig. 4) . This in contrast to corresponding ice fields in ECMWF and climate models, as noticed in Li et al. (2005, 2007) and Eriksson et al. (2007a). Figures 6 and 7 show that the ice mass over these areas has a clear annual cycle, with minimum during the JJA season and maximum around the DJF season. The DJF maximum is most pronounced in the MLS data. The analysis in Li et al. (2005) was performed for January 2005, based on same MLS data as used here. A more detailed analysis of the data sets reveals strong diurnal variations for these areas (Eriksson et al., 2007b), and this can cause differences in mean value between SMR and CloudSat/MLS (flying in tandem, as part of the A-train satellite set). Diurnal variations are much less pronounced over the oceans.

3.4 Probability density functions

Deeper insight into the performance of the different retrievals can be obtained by comparing probability density functions (PDF). That is, the relative occurrence rate of different pIWP values, with respect to the total number of data points. This implies comparison on single measurement basis and some additional considerations are needed. For example, instrumental noise should have little influence on seasonal means for all three instruments, but will cause differences in PDF for lower pIWP. Only values above 4 g/m^2 are considered in PDFs for this reason. This value matches the estimated detection threshold for Odin-SMR, and the other instruments are better in this respect, particularly CloudSat.

A more critical consideration is differences in horizontal resolution. This is illustrated in Fig. 8, where PDFs for CloudSat data averaged over different distances are displayed. The frequency of lower pIWPs increases with size of averaging window. The reversed, and largest, impact is found for highest pIWP, showing that such pIWP values are normally confined to smaller areas. This observation gives perspective to the beam filling simulation reported in Sect. 3.2.

PDFs for complete data sets are compared in Fig. 9. No important differences were found when restricting the MLS and SMR data to the season covered by the CloudSat measurements available (as for Fig. 4). An excellent agreement is found between CloudSat and SMR, except for the lowest and highest pIWP. The higher PDF at low pIWP for SMR can indicate false cloud detections, caused by the random calibration error reported by Ekström et al. (2007). The beam filling effect for low ΔT_b originating in the PSD (Sect. 3.2) can also be involved. The cloud inhomogeneity correction for SMR (Sect. 3.2) changes the PDF above ≈150 g/m^2. The CloudSat PDF is largely found between the two SMR PDFs. This could be taken as an indication on that a lower value for the maximum correction shall be applied for SMR. A maximum correction of 4% (instead of 10%) gives also same mean as CloudSat for seasonally matched data. However, the CloudSat PDF is for the provisional R03 data product relatively uncertain

at higher ice masses, and this option for tuning the SMR beam filling correction was rejected.

The MLS PDF deviates from the others. A possible reason for this behaviour is the larger footprint of MLS. A rough estimate of this effect is provided by the 40 s averages in Fig. 8. Complete agreement can not be expected as the simple averaging of CloudSat does not manage to mimic all properties of the MLS limb sounding measurements, but a limitation to values below 200 g/m^2 is found in both cases. The linear mapping from T_{cir} to IWC applied in MLS V1.5 retrievals also affects the PDF. The MLS PDF is not discussed further here as a detailed comparison between IWC PDFs for MLS V2.2 data and CloudSat is made in Wu et al. (2007)[1].

Comparison with ARM tropical ground-based radar measurements is made in Fig. 10. The ARM radars are placed in the equatorial western part of the Pacific Ocean. This is an area characterised by high sea surface temperatures and associated high convection. Mean pIWP values are accordingly higher for Fig. 10 than for complete SMR and CloudSat datasets. More precisely, the means are 6.14, 7.65 and 9.51 g/m^2 for CloudSat, ARM and SMR, respectively. Main differences are found above 100 g/m^2, where the ARM PDF is consistently above the CloudSat one. The ARM data also contain cases with pIWP above 500 g/m^2 values totally lacking for SMR and CloudSat. The SMR PDF suffers from a small statistical ensemble and is noisy, but is on average above the ARM PDF.

4 Summary and conclusions

Data from first official Odin-SMR, Aura MLS and CloudSat microwave cloud ice retrievals have been compared. The comparison follows the SMR retrievals, and MLS and CloudSat ice water content profiles are weighted to obtain a partial ice column (pIWP) starting at ≈11 km (Fig. 1). Only latitudes inside ±30° have been considered.

The instrument with the least complicated error budget is CloudSat. This as the spatial resolution of SMR and MLS is much poorer, resulting in two main considera-

tions. Firstly, inhomogeneities of the ice field over the antenna footprint combined with a non-linear relationship between ice mass and measured signal, cause a retrieval uncertainty denoted as the beam filling problem. This effect was studied for SMR and found to have a smaller impact than speculated in Eriksson et al. (2007a), and the correction function applied was updated accordingly. MLS measurements were estimated to be less influenced by beam filling than SMR. Secondly, the poorer vertical resolution of MLS and SMR gives a possible ambiguity in the altitude of observed cloud ice mass.

All the retrievals involve assumptions concerning the particle size distribution (PSD). It is shown that the resulting retrieval uncertainty should be relatively similar between the instruments, particularly for MLS and SMR that both apply the PSD of McFarquhar and Heymsfield (1997). Microwave techniques are primarily sensitive to the particle fraction having the largest size and the amount of small particles is estimated by an extrapolation of measurement information using assumed PSD. This effect was not studied in any quantitative manner, but we have argued that the various assumptions made in the different retrievals could lead to CloudSat yielding lower values than MLS and SMR.

Geographical regions with very low mean values coincide very well between the instruments, and match the general expectations on areas with a low amount of high clouds. This indicates that none of the retrievals suffers of a significant degree of false cloud detections. This, combined with a similar dynamic range of the retrievals in terms of pIWP, give a consistent view on geographical distribution of the cloud ice mass. However, there are substantial differences in overall retrieved mean values.

Comparable mean values for CloudSat and MLS are 2.12 and 4.30 g/m^2, respectively. This difference is only marginally influenced by uncertainties around the vertical response of SMR. Inclusion of correction for beam filling should increase the MLS mean. The same applies to the improved (non-linear) mapping from cloud induced radiance to IWC applied in a newly activated MLS V2.2 retrieval version, that anyhow mainly affects altitudes lower than considered here (Wu et al., 2007[1]). This leaves two main explanations for the found difference: 1. Different PSD assumptions. 2. An

upward shift of cloud ice masses in MLS retrievals. There are indications that MLS retrievals give cloud top altitudes with a ≈1 km positive bias (Wu et al., 2007[1]), and it was found that such a shift of complete IWC profiles largely explains the difference to CloudSat discussed.

Odin-SMR mean values, consistent with both CloudSat and MLS, can be obtained by applying different corrections for cloud inhomogeneity. No correction gives a SMR mean of 1.95 g/m^2. A maximum correction of 4% was found to give data very similar to CloudSat, with respect to both mean value and pIWP probability density function. The correction function suggested in Eriksson et al. (2007a) and the updated version give 4.19 and 2.69 g/m^2, respectively, where the latter value shall be taken as best estimate for SMR.

If the span of values given above are used as an overall error estimation, mean pIWP for considered season is found to be 3.1 ±1.2 g/m^2. This retrieval accuracy on the order of 40% can potentially be decreased by future retrieval versions, where the problems discussed above are better addressed. On the other hand, such an accuracy must be judged as good in comparison to the high spread of cloud ice masses among climate models found by John and Soden (2006), and datasets considered should constitute good a validation source for improving the parameterisation of cloud physic processes used in atmospheric models.

Acknowledgements. Financial support was provided by the Swedish Space Board and the Swedish National Graduate school of Space Technology. The Odin cloud ice dataset is based on essential contributions from the Odin-SMR retrieval group and the ARTS community.

References

Davis, C. P., Evans, K. F., Buehler, S. A., Wu, D. L., and Pumphrey, H. C.: 3-D polarised simulations of space-borne passive mm/sub-mm midlatitude cirrus observations: a case study, Atmos. Chem. Phys., 7, 4149–4158, 2007, http://www.atmos-chem-phys.net/7/4149/2007/. 12039, 12046

Dessler, A. E. and Yang, P.: The distribution of tropical thin cirrus clouds inferred from Terra MODIS data, J. Climate, 16, 1241–1247, 2003. 12037

Ekström, M., Eriksson, P., Rydberg, B., and Murtagh, D. P.: First Odin sub-mm retrievals in the tropical upper troposphere: humidity and cloud ice signals, Atmos. Chem. Phys., 7, 459–469, 2007, http://www.atmos-chem-phys.net/7/459/2007/. 12038, 12040, 12050

Eriksson, P., Ekström, M., Rydberg, B., and Murtagh, D. P.: First Odin sub-mm retrievals in the tropical upper troposphere: ice cloud properties, Atmos. Chem. Phys., 7, 471–483, 2007a. 12038, 12040, 12041, 12045, 12046, 12047, 12049, 12052, 12053, 12057, 12059

Eriksson, P., Rydberg, B., Ekström, M., and Murtagh, D. P.: Combining Odin-SMR and A-train cloud ice information, in: EarthCARE workshop, ESA/ESTEC, Noordwijk, The Netherlands, 7–9 May, 2007b. 12049

Evans, K. F. and Stephens, G. L.: Microwave radiative transfer through clouds composed of realistically shaped ice crystals. Part II : Remote sensing of ice clouds, J. Atmos. Sci., 52, 2058–2072, 1995. 12037

Evans, K. F., Walter, S. J., Heymsfield, A. J., and Deeter, M. N.: Modeling of submillimeter passive remote sensing of cirrus clouds, J. Appl. Meteorol., 37, 184–205, 1998. 12037

Heymsfield, A. J. and McFarquhar, G. M.: Cirrus, chap. Mid-latitude and tropical cirrus: microphysical properties, Oxford University Press, Inc., New York, 78–101, 2002. 12039

Hong, G., Heygster, G., Miao, J., and Kunzi, K.: Detection of tropical deep convective clouds from AMSU-B water vapor channels measurements, J. Geophys. Res., 110, D05205, doi:10.1029/2004JD004949, 2005. 12038

Jarnot, R. F., Perun, V. S., and Schwartz, M. J.: Radiometric and spectral performance and calibration of the GHz bands of EOS MLS, IEEE Trans. Geosci. Remote Sensing, 44, 1131–1143, 2006. 12041

John, V. O. and Soden, B. J.: Does convectively-detrained cloud ice enhance water vapor feedback?, Geophys. Res. Lett., 33, L20701, doi:10.1029/2006GL027260, 2006. 12037, 12053

Li, J. L., Waliser, D. E., Jiang, J., Wu, D. L., Read, W., Waters, J. W., Tompkins, A. M., Donner, L. J., Chern, J. D., Tao, W. K., Atlas, R., Gu, Y., Liou, K. N., Genio, A. D., Khairoutdinov, M., and Gettelman, A.: Comparisons of EOS MLS cloud ice measurements with ECMWF analyses and GCM simulations: Initial results, Geophys. Res. Lett., 32, L18710, doi:10.1029/2005GL023788, 2005. 12038, 12049

Li, J. L., Jiang, J., Waliser, D. E., and Tompkins, A. M.: Assessing consistency between EOS MLS and ECMWF analyzed and forecast estimates of cloud ice, Geophys. Res. Lett., 34, L08701, doi:10.1029/2006GL029022, 2007. 12038, 12049

Liu, C. L. and Illingworth, A.: Toward more accurate retrievals of ice water content from radar measurements of clouds, J. Appl. Meteorol., 30, 1130–1146, 2000. 12044

McFarquhar, G. M. and Heymsfield, A. J.: Parameterization of tropical cirrus ice crystal size distribution and implications for radiative transfer: Results from CEPEX, J. Atmos. Sci., 54, 2187–2200, 1997. 12041, 12042, 12046, 12052, 12058

Murtagh, D., Frisk, U., Merino, F., Ridal, M., Jonsson, A., Stegman, J., Witt, G., Eriksson, P., Jiménez, C., Megie, G., de La Noë, J., Ricaud, P., Baron, P., Pardo, J. R., Hauchcorne, A., Llewellyn, E. J., Degenstein, D. A., Gattinger, R. L., Lloyd, N. D., Evans, W. F. J., McDade, I. C., Haley, C., Sioris, C., von Savigny, C., Solheim, B. H., McConnell, J. C., Strong, K., Richardson, E. H., Leppelmeier, G. W., Kyrölä, E., Auvinen, H., and Oikarinen, L.: An overview of the Odin atmospheric mission, Can. J. Phys., 80, 309–319, 2002. 12040

Stephens, G. L., Vane, D. G., Boain, R. J., Mace, G. G., Sassen, K., Wang, Z. E., Illingworth, A. J., O'Connor, E. J., Rossow, W. B., Durden, S. L., Miller, S., Austin, R. T., Benedetti, A., and Mitrescu, C.: The CloudSat mission and the A-train – A new dimension of space-based observations of clouds and precipitation, B. Am. Meteor. Soc., 83, 1771–1790, 2002. 12038, 12043

Su, H., Read, W. G., Jiang, J. H., Waters, J. W., Wu, D. L., and Fetzer, E. J.: Enhanced positive water vapor feedback associated with tropical deep convection: New evidence from Aura MLS, Geophys. Res. Lett., 33, L05709, doi:10.1029/2005GL025505, 2006a. 12038

Su, H., Waliser, D. E., Jiang, J. H., Li, J. L., Read, W. G., Waters, J. W., and Tompkins, A. M.: Relationships of upper tropospheric water vapor, clouds and SST: MLS observations, ECMWF analyses and GCM simulations, Geophys. Res. Lett., 33, L22802, doi:10.1029/2006GL027582, 2006b. 12038

Waters, J. W., Froidevaux, L., Harwood, R. S., Jarnot, R. F., Pickett, H. M., Read, W., Siegel, P. H., Cofield, R. E., Filipiak, M. J., Flower, D. A., Holden, J. R., Lau, G. K., Livesey, N. J., Manney, G. L., Pumphrey, H. C., Santee, M. L., Wu, W. L., Cuddy, D. T., Lay, R. R., Loo, M. S., Perun, V. S., Schwartz, M. J., Stek, P., Thurstans, R. P., Boyles, M. A., Chandra, K. M., Chavez, M. C., Chen, G. S., Chudasama, B. V., Dodge, R., Fuller, R. A., Girard, M. A., Jiang, J. H., Jiang, Y. B., Knosp, B. W., LaBelle, R., Lam, J. C., Lee, K. A., Miller, D., Oswald, J. E., Patel, N. C., Pukala, D. M., Quintero, O., Scaff, D. M., Snyder, W. V., Tope, M. C., Wagner, P.,

and Walch, M.: The Earth Observing System Microwave Limb Sounder (EOS MLS) on the Aura satellite, IEEE Trans. Geosci. Remote Sensing, 44, 1075–1092, 2006. 12041

Wu, D. L., Read, W. G., Dessler, A. E., Sherwood, S. C., and Jiang, J. H.: UARS/MLS cloud ice measurements: Implications for H_2O transport near the tropopause, J. Atmos. Sci., 62, 518–530, 2005. 12038, 12045

Wu, D. L., Jiang, J. H., and Davis, C. P.: EOS MLS cloud ice measurements and cloudy-sky radiative transfer model, IEEE Trans. Geosci. Remote Sensing, 44, 1156–1165, 2006. 12038, 12042, 12046

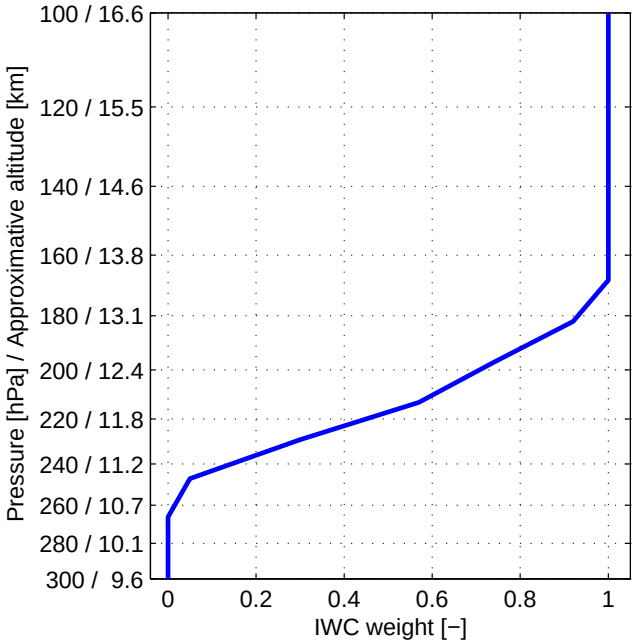

Fig. 1. Estimated vertical response of considered Odin-SMR retrievals. Profiles of IWC are converted to SMR partial IWP (pIWP) by weighting with the shown function, often denoted as the averaging kernel. The function is re-evaluated compared to Eriksson et al. (2007a). The analysis was here performed for conditions more relevant for the overall cloud ice mass.

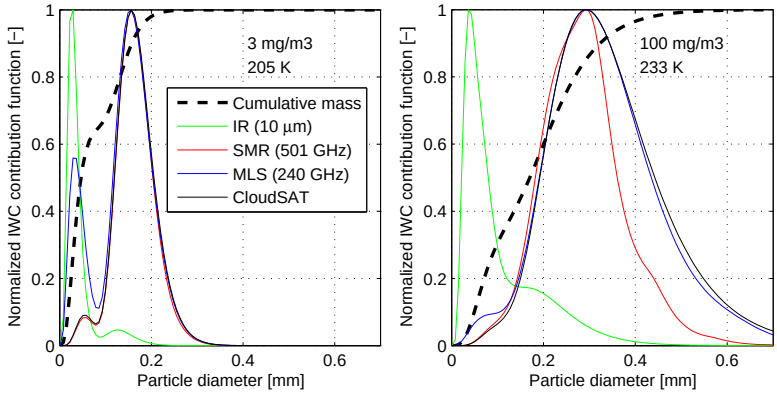

Fig. 2. Estimates of relative sensitivity to different particle sizes for some remote sensing instruments. Two combinations of IWC and temperature are considered: 3 mg/m^3 / 205 K (left) and 100 mg/m^3 / 233 K (right). Spherical particles and the PSD of McFarquhar and Heymsfield (1997) are assumed. Cumulative mass distributions are shown as dashed lines. The instrument responses are estimated as the product between PSD and the size-dependent cross-section. The complete extinction cross-section is considered for IR and MLS, only the scattering cross-section for SMR, and the backscattering cross-section for CloudSat. All functions are normalised with their maximum value. The figure shall only be interpreted in a schematic manner as no complete radiative transfer calculations are involved.

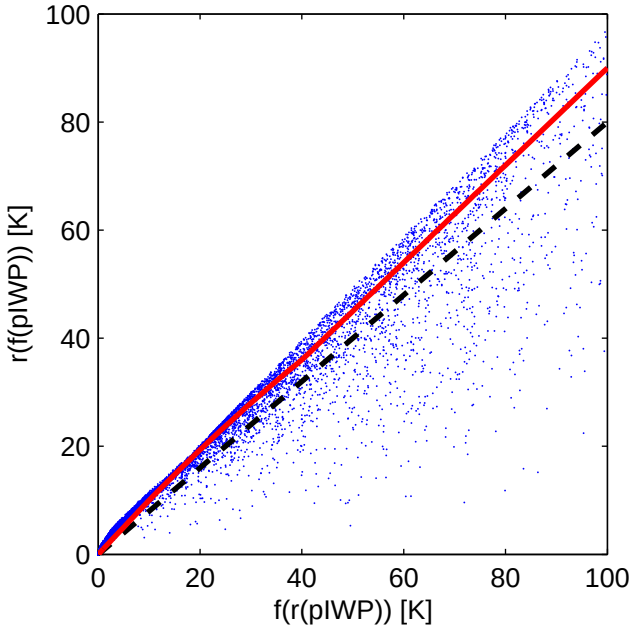

Fig. 3. Simple simulation of the beam filling effect for Odin-SMR. All available CloudSat data were considered, where 50 000 randomly selected data points are displayed here. The horizontal data dimension represents (1-D) retrieval assumptions made, while the vertical dimension aims at capturing real measurement conditions. The dashed (black) line corresponds to the correction function suggested in Eriksson et al. (2007a), while the solid (red) line is equivalent to the function selected here. Further details are given in the text.

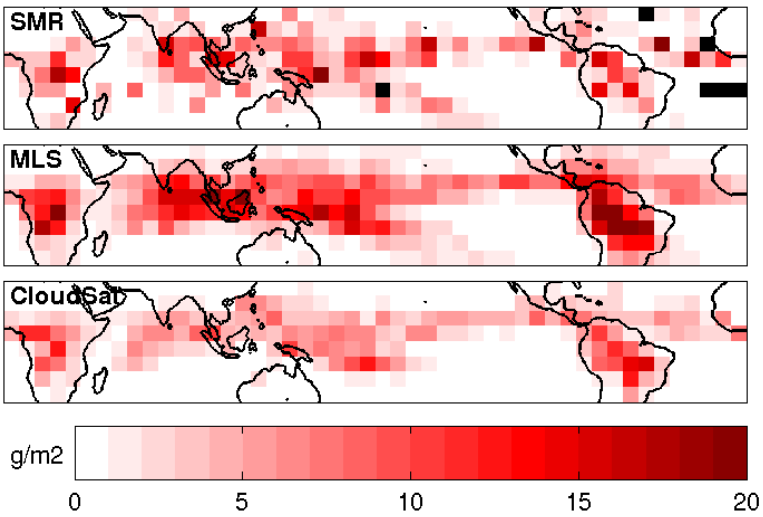

Fig. 4. Odin-SMR (top), Aura MLS (middle) and CloudSat (bottom) pIWP fields for data around 1 November . Data cover 15 October–15 November for Aura MLS (mean over 2004–2006) and CloudSat (2006), while for Odin-SMR the time period is 15 September–15 December (mean over 2001–2006). Black indicates less than 50 data points available for averaging and no IWP is given. Data averaged over 7.5° in both latitude and longitude.

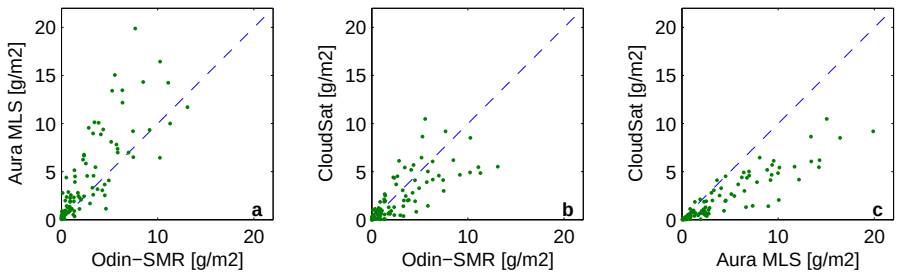

Fig. 5. Comparison of local mean values, between SMR and MLS **(a)**, between SMR and CloudSat **(b)**, and between MLS and CloudSat **(c)**. Data as in Fig. 4, but divided into areas with length of 15° in both latitude and longitude. The one-to-one relationship is given as a dashed line.

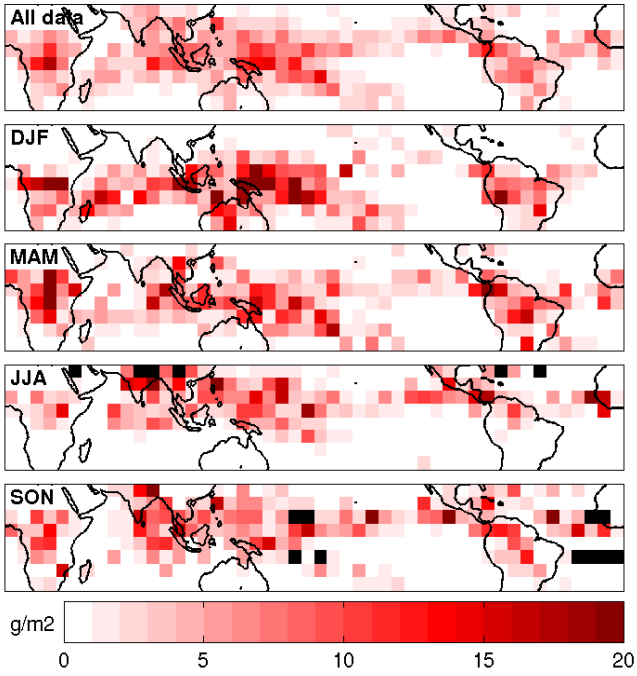

Fig. 6. Overall (top) and seasonal (lower four panels) mean pIWP fields for Odin-SMR. Data cover the period August 2001–September 2006. Black indicates less than 50 data points available for averaging and no IWP is given. Seasons are defined as: DJF = December–February, MAM = March–May, JJA = June–August, and SON = September–December.

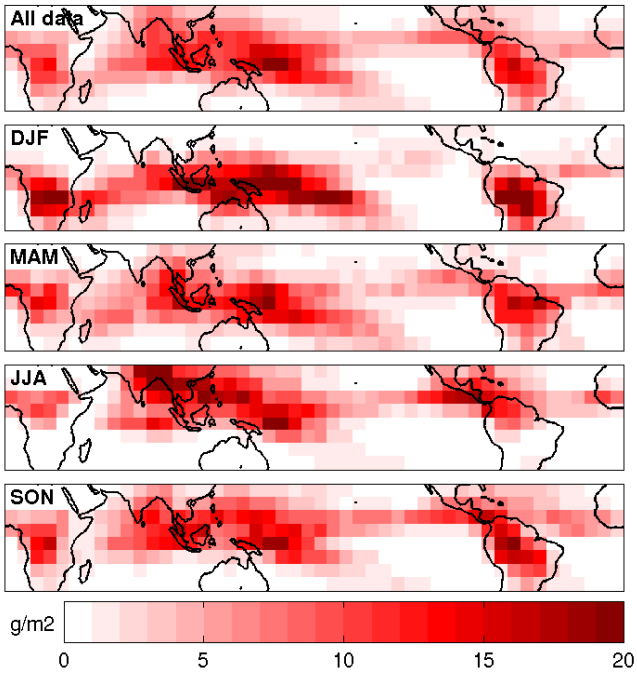

Fig. 7. Overall (top) and seasonal (lower four panels) mean pIWP fields for AURA MLS. Data cover the period August 2004–February 2007. Seasons are defined as in Fig. 6.

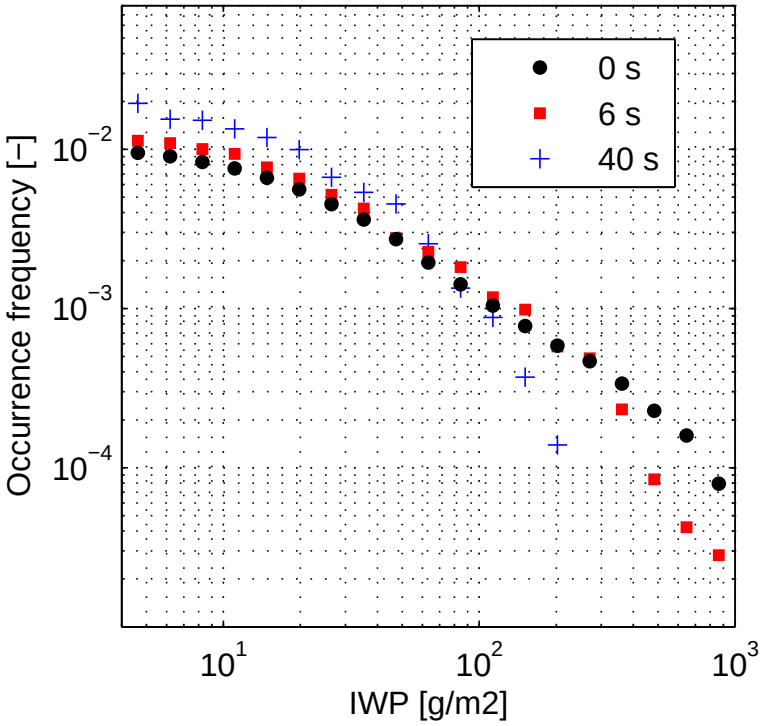

Fig. 8. Distribution of CloudSat pIWP values when averaged over different time windows. One second corresponds to a horizontal distance of ≈7.5 km.

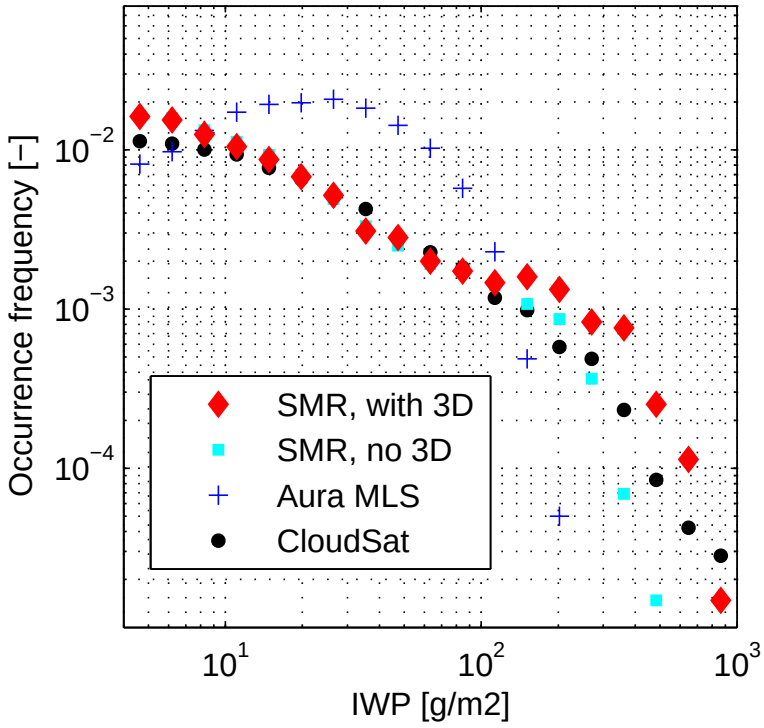

Fig. 9. Distribution of IWP values for complete Aura MLS, Odin-SMR and CloudSat data sets. For Odin-SMR data are shown with and without correction for cloud inhomogeneity. CloudSat data are shown for 6 s averaging, to roughly match the SMR footprint.

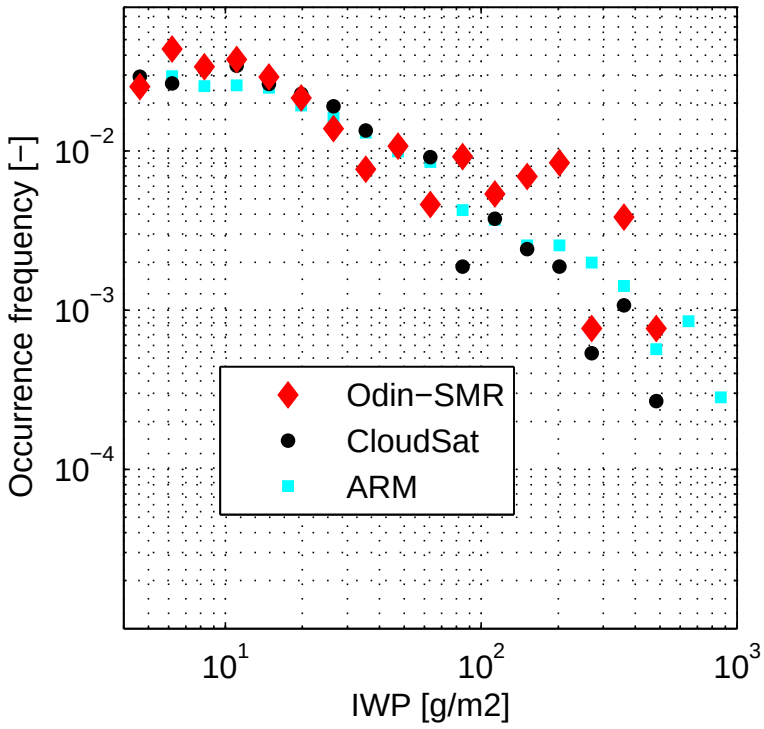

Fig. 10. Comparison of pIWP distributions from an area around the tropical ARM stations. Satellite data are taken from a rectangular area, limited of latitudes –9° and 11° and longitudes 142° and 172°. Selection of SMR and ARM data are further restricted to the time period 15 September–15 December (all available years included).